Polymorphism and electronic structure of polyimine and its potential significance for prebiotic chemistry on Titan

Martin Rahm[a,1], Jonathan I. Lunine[b,c,1], David A. Usher[a], and David Shalloway[d]

[a]Department of Chemistry and Chemical Biology, Cornell University, Ithaca, NY 14853; [b]Department of Astronomy, Cornell University, Ithaca, NY 14853; [c]Carl Sagan Institute, Cornell University, Ithaca, NY 14853; and [d]Department of Molecular Biology and Genetics, Cornell University, Ithaca, NY 14853

The chemistry of hydrogen cyanide (HCN) is believed to be central to the origin of life question. Contradictions between Cassini–Huygens mission measurements of the atmosphere and the surface of Saturn's moon Titan suggest that HCN-based polymers may have formed on the surface from products of atmospheric chemistry. This makes Titan a valuable "natural laboratory" for exploring potential nonterrestrial forms of prebiotic chemistry. We have used theoretical calculations to investigate the chain conformations of polyimine (pI), a polymer identified as one major component of polymerized HCN in laboratory experiments. Thanks to its flexible backbone, the polymer can exist in several different polymorphs, which are relatively close in energy. The electronic and structural variability among them is extraordinary. The band gap changes over a 3-eV range when moving from a planar sheet-like structure to increasingly coiled conformations. The primary photon absorption is predicted to occur in a window of relative transparency in Titan's atmosphere, indicating that pI could be photochemically active and drive chemistry on the surface. The thermodynamics for adding and removing HCN from pI under Titan conditions suggests that such dynamics is plausible, provided that catalysis or photochemistry is available to sufficiently lower reaction barriers. We speculate that the directionality of pI's intermolecular and intramolecular =N–H···N hydrogen bonds may drive the formation of partially ordered structures, some of which may synergize with photon absorption and act catalytically. Future detailed studies on proposed mechanisms and the solubility and density of the polymers will aid in the design of future missions to Titan.

hydrogen cyanide | prebiotic chemistry | Titan | polymers

Saturn's moon Titan is a carbon-rich, oxygen-poor world with a wide range of organic compounds, atmospheric energy sources, and alkane liquid seas—all measured by the remarkably successful Cassini–Huygens mission (1). The extreme cold puts liquid water out of reach—buried 50–100 km below a frigid ice crust (2). The lack of liquid water and presence of liquid hydrocarbons makes Titan a unique "natural laboratory" for exploring potential nonterrestrial forms of prebiotic chemistry or, more speculatively, biochemistry, whose essential biopolymers would differ profoundly from terrestrial ones (3). Regardless of the specific chemistry involved, life requires polymorphic molecules that combine flexibility with the ability to form the organized metastable structures needed for function, adaptation, and evolution. This, almost certainly, requires extended molecules capable of intermolecular and intramolecular hydrogen bonding, but such bonds need not involve oxygen; nitrogen is a potential surrogate. Although =N–H···N bonds are weaker than those involving oxygen, their energies are large compared with thermal energy ($kT \sim 0.18$ kcal/mol at Titan's low temperature, 90–94 K) and intermolecular and intramolecular bonds need not compete with the strong –O–H···O hydrogen bonds in water, as on Earth. Thus, they might provide the needed balance between rigidity and polymorphism.

Chemistry in Titan's atmosphere, which is primarily nitrogen with an admixture of methane, is driven by solar-UV photons and energetic particle radiation to produce hydrocarbons and nitrogen-bearing organics. Cassini–Huygens mission data show that the most abundant nitrogen-bearing product of the atmospheric chemistry is hydrogen cyanide (HCN) (4), which is expected to condense into aerosols that drift down to land and sea. However, HCN has not been observed to be present on Titan's surface (5); instead, features tentatively identified as consistent with acetonitrile (CH_3CN) and cyanoacetylene (HC_3N) are observed with the Cassini visible and infrared mapping spectrometer (VIMS). The interpretations of the VIMS spectra in terms of specific non-HCN molecules are reported by Clark et al. (5) as "possible but not definitive," because of the challenge of observing Titan's surface through the dense atmosphere and the limited resolution of the instrument. The data do not contradict the view that some or all of the signature is coming from polymers formed from HCN and, more generally, that chemistry on the surface is transforming HCN into other molecules and polymers.

HCN is present in comets (6) and is believed to be a key precursor to the origin of life (7–11). Previous studies have focused on its capability for abiotic synthesis of oxygen-containing molecules (e.g., amino acids and polypeptides), but not on the types of prebiotic chemistry that might occur in oxygen-poor environments. This, combined with the possibility of experimental tests in future exploratory missions to Titan, motivates a deeper understanding of the structure and behavior of HCN polymers and their potential chemistry on Titan.

Using solution-state multidimensional NMR, He et al. (12) found that 75% of the HCN-based polymers formed in laboratory

---

Significance

Titan is the only place in the solar system, except Earth, where rainfall and seasonally flowing liquids erode the landscape. Whereas the surface pressure is similar to that of Earth, the temperature is extremely low and the dominant liquids are methane and ethane. This makes Titan a test case for exploring the environmental limits of prebiotic chemistry and addressing the question of whether life can develop without water. Experimental and observational data suggest that hydrogen cyanide, the most abundant hydrogen-bonding molecule in Titan's atmosphere, may polymerize on the surface to polyimine. Using quantum mechanical calculations, we show that polyimine has interesting electronic and structural properties that could potentially facilitate prebiotic chemistry under cryogenic conditions akin to those on Titan.
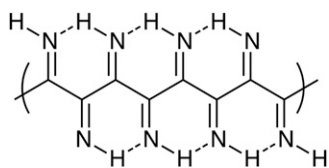

Fig. 1. Lewis structure representation of pI. A flexible single-bonded carbon backbone and complementary intrachain and interchain hydrogen bonding allow for multiple competing 1D conformations and 3D polymorphs.

experiments were polyimine (pI) (Fig. 1). These have a flexible C–C bonded backbone and =NH groups that provide for interchain and intrachain hydrogen bonding. These polymers may be present on Titan and escaped detection thanks to observational conditions that make it difficult to identify them spectroscopically (5). Not much is known about them; the only theoretical studies, conducted decades ago, were of isolated polymers and dimers, and used methodologies whose accuracy is now greatly surpassed (13, 14). This contrasts with substituted polyimines/poly-isocyanides, whose synthesis and conformation have been extensively studied experimentally, in part because their helical structures gives them practical and potential importance in electronics, biosensing, and tailored catalysis (14–16).

Here, we use density functional theory (DFT) to computationally explore potential polymorphs (conformations) and the electronic structure of pI. A striking coupling between conformation

and electronic band gap is identified, indicating that pI may be able to absorb a wide spectrum of photons, including those available at Titan's surface. This source of energy could potentially be used to catalyze chemistry relevant to prebiotic evolution, even in the absence of water.

Results

The potential conformational space of pI is large. We have used a combination of plane-wave–based DFT and structure prediction algorithms and molecular calculations of isolated 20-mer models to explore a small but illustrative subset of polymorphs, differentiated primarily by their carbon backbone N=C–C=N dihedral angles. Starting from the extreme of a planar chain, we computationally scanned increasingly coiled conformations, thereby exploring the most important degree of freedom governing pI's structural and electronic properties (Fig. 2). Infinite chains were studied, and energies per unit HCN were computed and found to be close in energy for all of the polymorphs (~1–2 kcal/mol HCN; Table 1). We also calculated the packing of each chain in representative 3D lattices. The packed chains had lower energies due to the additional intermolecular =NH···N interactions, but the relative energies were still close. Moreover, the electronic structure was only marginally affected. Therefore, for clarity, we focus on the isolated chains.

Although the differences between the energies of the different polymorphs reach below the accuracy of the used DFT methodology, the results show that the thermodynamic and kinetic conformational flexibility allowed by the carbon–carbon single-bonded
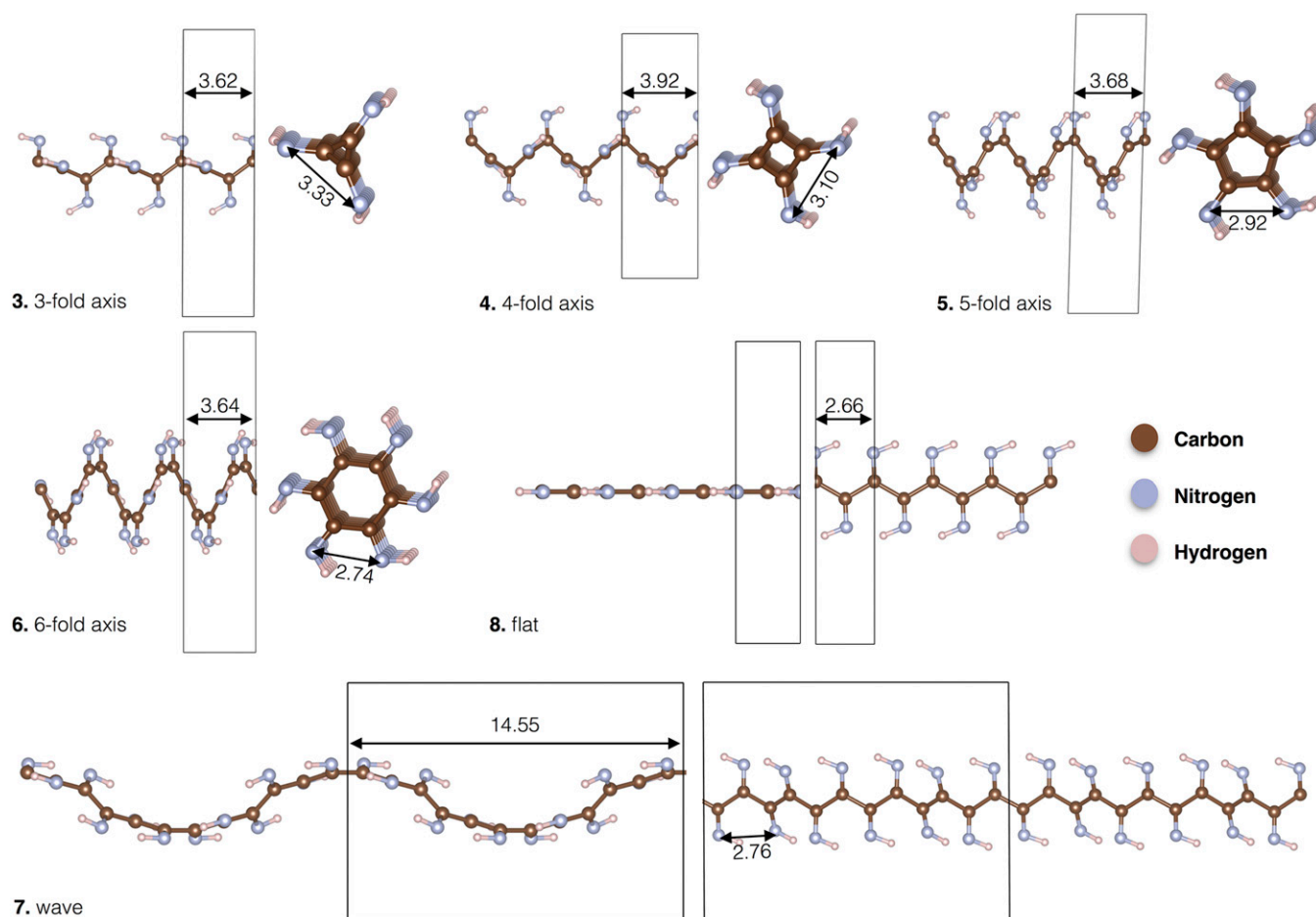

Fig. 2. Investigated polyimine single chains **3–8**. Unit cell width and nearest N–N distances are shown in angstoms.

Table 1. Calculated properties of HCN (1, 2) and 1D pI chains 3–8

Material	ΔE^*, kcal/mol	Band gap, eV	N=C–C=N dihedral angle, °
1. HCN (g)	17.8	—	—
2. HCN (s)	9.6	—	—
3. pI threefold helix	1.7	4.5	110
4. pI fourfold helix	2.4	4.3	68
5. pI fivefold helix	4.5	3.8	39
6. pI sixfold helix	2.1	3.5	26
7. pI wave	0.0	2.2	~3[†]
8. pI planar	0.8	1.5	0

*Energies per unit of HCN are from periodic HSE06 calculations, and are shown relative to the lowest energy structure **7**.
[†]Average value for all N=C–C=N dihedral angles in the unit cell.

backbone (Fig. 1) ensures that only disordered amorphous materials will be observed at Earth-ambient temperatures (even if, hypothetically, the polymers were completely monodisperse). At Titan's much lower surface temperature, however, specific polymorphs of the polymer might dominate and even crystallize. As we show below, the span of properties exhibited by these individual polymorphs are nothing short of remarkable—each having its own electronic, optical, and mechanical properties.

We can speculate that, in addition to relying on =N–H···N hydrogen bonding, any prebiotic processes on Titan might benefit, to some degree, from the dynamic making and breaking of covalent bonds. This would be advantageous for the assembly of primary structures (polymers) of reasonably low dispersity. Because of the low temperature, the first step in gauging the plausible existence of any such processes on Titan is finding a system with near-equilibrium thermodynamics for polymerization and depolymerization.

We have estimated the heat of reaction for pI polymerization, $pI(\infty) + 1$ HCN $\rightarrow pI(\infty)$, in the condensed phase, $\Delta H_{r,90K} = -5.6$ kcal/mol HCN, using a thermodynamic cycle detailed in *SI Appendix*. The cycle corrects accurate gas phase calculations with experimentally known heats of sublimation of HCN ($\Delta H_{sub}^0 = 9.0$ kcal/mol) and calculated energies of sublimation/interaction of the infinite chains [$\Delta E_{pI(s)\rightarrow pI(g)} \sim 1$ kcal/mol HCN]. $\Delta H_{r,90K} = -5.6$ is not exact, but we believe it offers a reasonable approximation to pI chain propagation in the solid state, or on surfaces where HCN monomers are hydrogen bonded before reaction. The Gibbs energy, $\Delta G_{r,90K}$, will be closer to zero still, due to the negative entropy associated with polymerization. The relevant activation barrier is unknown; however, it may be significantly reduced by tunneling, catalysis, photoexcitation (Fig. 3), or a combination of all three. If the thermodynamics of polymerization, <5 kcal/mol, were to represent the kinetic barrier to depolymerization of pI, reactions that shuffled polymer connectivity could proceed within seconds on Titan, thereby allowing for a dynamic chemical environment. HCN is from this aspect markedly different from the formally isoelectronic, and thermodynamically irreversible [$\Delta H_r = -40$ kcal/mol (17)] polymerization of acetylene to polyacetylene, which might also occur on Titan.

It is beyond the scope of the present work to undertake studies of explicit reaction mechanisms or processes that may allow for such dynamics. We would, however, like to point to a few possibilities. What is most striking about pI is the multitude of different hydrogen-bonded networks possible both within and in-between polymer chains. Fig. 4*A* highlights a triad of =NH groups capable of both donating and accepting hydrogen bonds, a structural unit not markedly different from an "oxyanion hole" situated in the active site of many enzymes (18). In enzymes, closely spaced oxyanion holes are known to work in tandem to stabilize transition states of different steps in a chemical transformation (19). Similar structural motifs are common in various man-made bioinspired catalysts (20, 21). The different polymorphs we have considered demonstrate that the alignment of =NH groups can generate large dielectric moments. This is intriguing for many reasons: electrostatic preorganization is known to occur in many enzymes and believed to be key to their catalytic function (22). Structures such as that shown in Fig. 4*A* might thus be catalytically active, and facilitate prebiotic reaction chemistry on Titan.

Quantum tunneling is another possibility. It can be important for cryogenic reactivity (23), including astrochemistry (24) and even biochemistry (25), and could play a role in allowing for chemistry on the surface of Titan.

Photon capture may provide activation energy for, and thereby synergize with, such catalytic mechanisms. A key question is whether pI can absorb photons at the wavelengths available on Titan, and analyzing the electronic structure of pI (Fig. 4 *C–E*) permits consideration of possible photon-induced low-temperature reactivity of the different polymorphs.

The electronic structure of polymorph **8** predicts it to have a band gap of 1.5 eV, which corresponds to a maximum light absorption in the 830 nm (infrared) range. From this minimum, increasing of the N=C–C=N dihedral angle widens the band gap, causing higher energy photons of visible and later UV wavelengths to be absorbed instead. The lowest energy structure, **7**, is predicted to
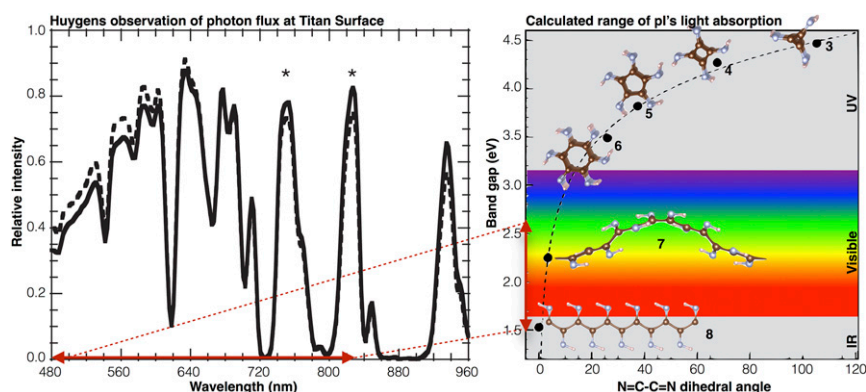

Fig. 3. Calculated band gaps of different polymer conformations provide a first approximation to their light absorption maximum (*Right*). The band gaps of pI polymorphs span a range of 3 eV and absorb across the entire visible spectrum and into the UV. The lowest energy conformation **7** is estimated to absorb in a region of relative transparency on Titan (*Left*). Photons of wavelengths below 480 nm were not measured by Huygens. (Left image reprinted with permission from ref. 26.)
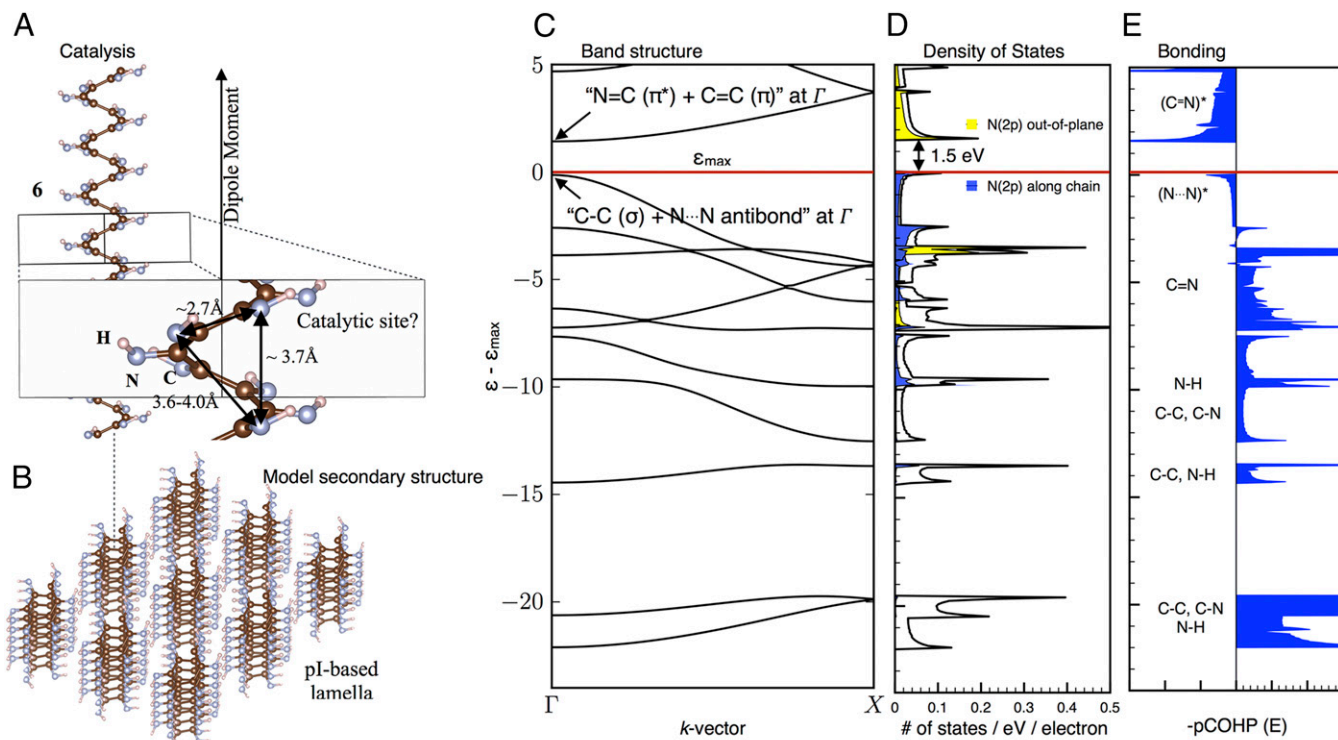
Fig. 4. (*A*) Chain **6** illustrates that "oxyanion hole"-like catalytic centers, a common feature of many enzymes, is a structural feature of pI. The ability of some conformations to generate electric fields by the alignment of =NH groups may give rise to dynamic materials capable of catalysis via electrostatic pre-organization. (*B*) Predicted 3D lattice of polymorph **6**, viewed to resemble a 2D lamella built by individual oligomers. (*C*) Band structure of planar pI **8** along the (0.0,0.0,0.0) → (0.5,0.0,0.0) path in the first Brillouin zone. ε_{max} denotes the top of the valence band. (*D*) Density of states showing a band gap of 1.5 eV, approximating light absorption in the 830-nm infrared region. The charge density projected onto out-of-plane and along-chain atomic 2p-functions on nitrogen are shown in yellow and blue, respectively. (*E*) Projected crystal orbital Hamilton population (pCOHP) bonding analysis of nearest neighbors, reveals a small antibonding N⋯N interaction at the top of the valence band. This explain the energetic preference for the curved structure **7** ahead of the planar structure **8**. The bottom of the conduction band is predominately C=N antibonding, indicating that photon absorption might activate protruding =N–H groups for reactivity and catalysis.

absorb yellow light in the 560 nm (2.2 eV) region. It is easy to realize how numerous other chain configurations may enable pI to access wavelengths across the entire 3-eV range laid out between the extremes **3** and **8**. Fig. 3 compares the calculated range of possible pI photon absorption with wavelengths corresponding to regions of relative transparency in Titan's atmosphere where more photons reach the surface.

How can we understand the remarkable structure–function relationship of pI? Fig. 4*C* displays how the lowest conduction band runs up (from $\Gamma \rightarrow X$), not down as expected from a nitrogen-π* band at the zone center Γ. This is due to concurrent C–C π-bonding at Γ, which weakens as we move $\Gamma \rightarrow X$. The density of states of chain **8** in Fig. 4*D* have been projected onto individual orbital contributions, namely the out-of-plane and along-chain directional 2p orbitals on nitrogen. The nitrogen 2p levels dominate the top of the valence band and most of the bottom of the conduction band, where carbon 2p also contributes slightly. This explains why changes in the N=C–C=N dihedral angle affect the overlap of adjacent p orbitals, which in turn modulate the band gap of pI (Fig. 3). Together with the projected crystal orbital Hamilton population (pCOHP) bonding analysis shown in Fig. 4*E*, it tells us two things: first, partial occupation of the lowest conduction band weakens C–N bonds and strengthens the C–C backbone. Occupation of the conduction band may occur both via chemical reduction or via photochemical excitation. Second, a small in-plane repulsion between adjacent nitrogen atoms does exists [in agreement with early predictions by Kollmar and Hoffmann (13)]; it is one reason for distortion from the planar geometry (e.g., **8** → **7**).

Speculations on the Implications of These Results for Life Without Water. A sine qua non of life is the formation of compartments allowing local entropy reduction. Although terrestrial biological compartmentalization is typically achieved using highly evolved protein shells (viruses) or bilamellar membranes (cells) that surround 3D volumes, localization of interacting molecules to (effectively) 2D compartments by polymer monolayers is a simpler possibility and could be important during the early stages of molecular evolution. The polarity and ability of pI polymers to form intermolecular hydrogen bonds suggests the possibility that they might form alkaphobic monolayers in Titan's alkane-rich environment—mirroring the hydrophobic Langmuir films formed by hydrocarbon polymers on Earth. The interaction strength of ~1 kcal/mol HCN between chains would be adequate to maintain such secondary structures once formed. At Titan's low temperatures, these would be solid; however, because of comparable energies of different chains conformations (Table 1), they could contain a mixture of ordered and disordered regions with enough defects to permit lateral migration and interactions between inserted smaller molecules. Stacked lamellae, like those formed in crystal melts, is another possibility (Fig. 4*B*). Small pI crystals or chain-folded lamellae formed during the sedimentation of atmospheric polymers (i.e., in processes analogous to melt cooling) might nucleate and template lamellar extension on Titan's surface. Possibilities like this, although consistent with the energetic and electronic calculations presented above, are very speculative and intended as a suggestion of the kinds of structures that might occur, rather than a specific prediction. Because they are impossible to form naturally in a warmer world containing water and oxygen, only future

exploratory missions to Titan can test the hypothesis that natural chemical systems evolve chemical complexity in almost any circumstance (3).

The larger seas of Titan have been determined by radar sounding to be mostly methane with significant admixtures (~10%) of ethane and nitrogen (27, 28). Because HCN is mostly insoluble in such mixtures (29), it is unlikely that polymers will form there. Rather, it is more likely that the materials investigated herein may undergo reactions in tidal pools near the shores of seas and lakes, where geological activity, tidal effects associated with Titan's noncircular orbit, and changes in the hemispherical distribution of sunlight caused by ~10^5-y variations in Saturn's orbit could provide a more dynamic environment (30, 31). Seasonal emptying and refilling of the smaller liquid "lakes," such as Ontario Lacus in the Southern Hemisphere, and longer-timescale variations in sea levels associated with Saturn's orbital variations, may allow cycling of these materials between liquid and dry (shoreline) environments, where they would be well positioned to undergo further chemistry. Although the densities of the investigated crystals in our work are in the range of 1.2–1.4 g/cm^3 (*SI Appendix*, Table S1), well above the expected density of Titan's seas (0.4–0.7 g/cm^3) (32), defects and lacunae might reduce the density enough to permit individual or stacked lamellae to float. Copolymerization with acetylene, or heterodispersion of polyacetylene, a somewhat related polymer [density of ~0.4 g/cm^3 (33)] in pI could further reduce the density.

Detection of the solid polymers on Titan will be difficult from remote sensing. Direct chemical analyses on the surface either in lakes and seas or on the adjacent shorelines by in situ techniques seems more promising, but will require sending an instrumented lander to Titan's surface (34). Laboratory studies of the solubility and density of pI and other related polymers will aid in the decision of whether to send such a probe to the seas—where targeting and sampling is easier—or to the technically more challenging shoreline/dry environments.

Implications for Chemistry, Functional Materials, and Catalysis.

Whereas we have framed this study from a planetary chemist's point of view, it is important to realize that different kinds of poly-isocyanides (poly-RNC, substituents R different from H) are of interest also in a more general sense. It has been established that the most common conformation of these polymers are fourfold sized helices (14–16). This contrasts with our results, which suggests that a wave conformation and the possibility of sheet structures become competitive when R=H. The sixfold conformation is also predicted to be of lower energy than the fourfold conformation that has been experimentally inferred with larger R groups. Structural properties such as helical pitch and handedness are of obvious importance in biology where α-helices and β-sheets have profound influence on biological activity. Different main-chain conformations can display different optical properties, and non–HCN-based chiral polyisocyanides, with either right-handedness or left-handedness, have been synthesized (15). The conformation–band gap connection shown in Fig. 4 is an extreme example of a structure–function relationship, and our results carry with them a suggestion of utility: The conformations of pI, consisting formally of hydrogen isocyanide units, may be valuable models for functional materials design. The purposeful design of ferroelectric materials that respond to external electric fields is one example. Consider, for instance, the alignments of local dipoles arising from =NH groups and how polarization is generated along the chain axis in **6** (Fig. 2), whereas this is not possible in **7** or **8**. Other examples include the design of nanowires for devices and, as we have speculated, chiral catalysts. This could be undertaken by chemically modifying (and rigidifying) a pI scaffold. Therefore, in addition to being of interest for prebiotic chemistry

in the outer solar system, the pI polymer holds promise as an instructive model material for the study of emergent properties, including semiconduction, ferroelectricity, and catalysis.

Materials and Methods

Extended Calculations. Extended DFT calculations were performed using the Vienna ab initio simulation package (VASP), version 5.3.5 (35, 36). Geometries were optimized using the Predew–Burke–Ernzerhof (PBE) (37) generalized gradient approximation functional. Standard projected augmented wave potentials (36, 38) were used together with a plane-wave kinetic energy cutoff of 600 eV. Brillouin zone sampling was performed on Γ-centered k meshes with a reciprocal space resolution of at least $2\pi \times 0.03$ Å^{-1}. Energies and forces were converged to <1 meV per atom. For 1D chains, each chain was separated by >10 Å in the periodic calculation, and the k-mesh density refers to the length dimension along the chain. We used the Heyd–Scuseria–Ernzerhof (HSE06) (39, 40) screened-hybrid functional for final estimates to relative energies and band gaps. HSE06 has a reported mean absolute error of 0.2 eV for band gaps (41).

Structure Searching. Chain conformations and 3D lattices were surmised by a hybrid approach: chain conformations corresponding to structures **5** and **7** were identified by geometric optimization of manually constructed molecular 20-mer structures. Molecular calculations were performed using the hybrid ωB97X-D (42) density functional in conjunction with a 6-31+G(d,p) basis set, as implemented in Gaussian 09 revision D01 (43). ωB97X-D is a general-purpose DFT functional with demonstrated high accuracy for thermochemistry for main group elements. Optimized molecular structures were subsequently used to create input for periodic DFT calculations. Other chain conformations (**3**, **4**, and **6**) were identified by particle-swarm optimization (PSO) structure searches. The PSO searches were performed by coupling VASP with the CALYPSO code (44). Identification of representative 3D lattices of pI was possible following repeated PSO searches over the H$_1$C$_1$N$_1$ stoichiometry, while allowing for 1–6 units of HCN per unit cell. The final structures [1D chains **3–8** (Fig. 2) and select 3D lattices thereof (*SI Appendix*)] span a wide and representative range of N=C–C=N dihedral angles. A very large number of other conformations are, of course, also possible. The exact 3D structures are unlikely to represent the thermodynamic global minimum of the corresponding 1D chains in the condensed phase, but they do represent reasonable approximations to the influence of a chemical environment (~1 kcal/mol, HCN).

Thermal Corrections. The combined HSE06/PBE approach reasonably reproduces the National Institute of Standards and Technology experimental heat of sublimation of crystalline HCN ($\Delta H_{sub,calc}$, 7.4 kcal/mol, and $\Delta H_{sub,exp}$, 9.0 kcal/mol, determined between 202 and 254 °C), when corrections for thermal motion and consideration of rotational and translational degrees of freedom are included (the thermally noncorrected $\Delta E_{sub,calc}$ is 8.2 kcal/mol). Thermal corrections were obtained by phonon calculations, which proceeded following the calculation of tightly converged (1×10^{-8} eV/HCN) PBE geometries. Force constants were obtained through the direct method (45), i.e., from Hellmann–Feynman forces induced by small displacements introduced to a [5 × 5 × 5]-supercell of the HCN crystal unit cell, using the PHONOPY 1.9.7 code (46). Phonon calculations could not be performed on pI. Near free rotation around carbon–carbon bonds is implied by similar energies of many different conformers. This, in combination with the possibility of irrational helical pitches requires the use of large unit cells, which make such calculations prohibitively expensive. Analytical vibrational analyses on the molecular 20-mer models of **6**, **5**, and **7** did, however, identify those as true minima on the potential energy surface, which allowed for calculation of thermal and entropic (1 atm, 90 K) correction for the gas phase polymerization reaction.

Electronic Structure Analysis. pCOHP (47) bonding analyses and orbital projections of pI's density of state were done using the LOBSTER program (48).

SI Appendix. *SI Appendix* includes further comments on the electronic structure of pI, including frontier orbitals of select 20-mer models and band-decomposed charge densities of extended systems; summation of relative energies, structures and band gaps of 1D chains and corresponding 3D lattices, and *xyz* coordinates and unit cells of all structures considered; and description of the thermodynamic cycle used to approximate condensed-phase polymerization.

1. Bezard B, Yelle RV, Nixon CA (2014) The composition of Titan's atmosphere. *Titan: Interior, Surface, Atmosphere, and Space Environment*, eds Müller-Wodarg I, et al. (Cambridge Univ Press, Cambridge, UK), pp 158–189.
2. Beghin C, Sotin C, Hamelin M (2010) Titan's native ocean revealed beneath some 45 km of ice by a Schumann-like resonance. *C R Geosci* 342(6):425–433.
3. National Research Council (2007) *The Limits of Organic Life in Planetary Systems* (The National Academies Press, Washington, DC).
4. Lavvas PP, Coustenis A, Vardavas IM (2008) Coupling photochemistry with haze formation in Titan's atmosphere, Part I: Model description. *Planet Space Sci* 56(1):27–66.
5. Clark RN, et al. (2010) Detection and mapping of hydrocarbon deposits on Titan. *J Geophys Res Planets* 115:E10005.
6. Ehrenfreund P, Charnley SB, Wooden D (2004) From interstellar material to comet particles and molecules. *Comets II* (Univ of Arizona Press, Tucson, AZ).
7. Sutherland JD (2016) The origin of life—Out of the blue. *Angew Chem Int Ed Engl* 55(1):104–121.
8. Ruiz-Bermejo M, Zorzano M-P, Osuna-Esteban S (2013) Simple organics and biomonomers identified in HCN polymers: An overview. *Life (Basel)* 3:421–448.
9. Seckbach J (2005) *Origins: Genesis, Evolution and Diversity of Life* (Kluwer Academic Publishers, Dordrecht, The Netherlands).
10. Patel BH, Percivalle C, Ritson DJ, Duffy CD, Sutherland JD (2015) Common origins of RNA, protein and lipid precursors in a cyanosulfidic protometabolism. *Nat Chem* 7(4):301–307.
11. Oro J (1961) Mechanism of synthesis of adenine from hydrogen cyanide under possible primitive earth conditions. *Nature* 191(4794):1193–1194.
12. He C, Lin G, Upton KT, Imanaka H, Smith MA (2012) Structural investigation of HCN polymer isotopomers by solution-state multidimensional NMR. *J Phys Chem A* 116(19):4751–4759.
13. Kollmar C, Hoffmann R (1990) Polyisocyanides: Electronic or steric reasons for their presumed helical structure? *J Am Chem Soc* 112(13):8230–8238.
14. Clericuzio M, Alagona G, Ghio C, Salvadori P (1997) Theoretical investigations on the structure of poly(iminomethylenes) with aliphatic side chains. Conformational studies and comparison with experimental spectroscopic data. *J Am Chem Soc* 119(5):1059–1071.
15. Schwartz E, Koepf M, Kitto HJ, Nolte RJM, Rowan AE (2011) Helical poly(isocyanides): Past, present and future. *Polym Chem* 2(1):33–47.
16. van Buul AM, et al. (2013) Stiffness versus architecture of single helical polyisocyanopeptides. *Chem Sci (Camb)* 4(6):2357–2363.
17. Brothers EN, Izmaylov AF, Rusakov AA, Scuseria GE (2007) On calculating a polymer's enthalpy of formation with quantum chemical methods. *J Phys Chem B* 111(50):13869–13872.
18. Swiderek K, Marti S, Moliner V (2014) Theoretical study of primary reaction of Pseudozyma antarctica lipase B as the starting point to understand its promiscuity. *ACS Catal* 4(2):426–434.
19. Kursula P, Ojala J, Lambeir A-M, Wierenga RK (2002) The catalytic cycle of biosynthetic thiolase: A conformational journey of an acetyl group through four binding modes and two oxyanion holes. *Biochemistry* 41(52):15543–15556.
20. Linder M, Brinck T (2009) Synergistic activation of the Diels-Alder reaction by an organic catalyst and substituents: A computational study. *Org Biomol Chem* 7(7):1304–1311.
21. Zhou Y, et al. (2013) H-bonding activation in highly regioselective acetylation of diols. *J Org Chem* 78(22):11618–11622.
22. Kamerlin SCL, Sharma PK, Chu ZT, Warshel A (2010) Ketosteroid isomerase provides further support for the idea that enzymes work by electrostatic preorganization. *Proc Natl Acad Sci USA* 107(9):4075–4080.
23. Schreiner PR, et al. (2011) Methylhydroxycarbene: Tunneling control of a chemical reaction. *Science* 332(6035):1300–1303.
24. Goumans TPM, Kaestner J (2010) Hydrogen-atom tunneling could contribute to H2 formation in space. *Angew Chem Int Ed Engl* 49(40):7350–7352.
25. Masgrau L, et al. (2006) Atomic description of an enzyme reaction dominated by proton tunneling. *Science* 312(5771):237–241.
26. Tomasko MG, et al. (2005) Rain, winds and haze during the Huygens probe's descent to Titan's surface. *Nature* 438(7069):765–778.
27. Mastrogiuseppe M, et al. (2014) The bathymetry of a Titan sea. *Geophys Res Lett* 41(5):1432–1437.
28. Mitchell KL, Barmatz MB, Jamieson CS, Lorenz RD, Lunine JI (2015) Laboratory measurements of cryogenic liquid alkane microwave absorptivity and implications for the composition of Ligeia Mare, Titan. *Geophys Res Lett* 42(5):1340–1345.
29. Stevenson JM, et al. (2015) Solvation of nitrogen compounds in Titan's seas, precipitates, and atmosphere. *Icarus* 256:1–12.
30. Lorenz RD, Tokano T, Newman CE (2012) Winds and tides of Ligeia Mare, with application to the drift of the proposed time TiME (Titan Mare Explorer) capsule. *Planet Space Sci* 60(1):72–85.
31. Aharonson O, et al. (2009) An asymmetric distribution of lakes on Titan as a possible consequence of orbital forcing. *Nat Geosci* 2(12):851–854.
32. Hofgartner JD, Lunine JI (2013) Does ice float in Titan's lakes and seas? *Icarus* 223:628–631.
33. Saxman AM, Liepins R, Aldissi M (1985) Polyacetylene: Its synthesis, doping and structure. *Prog Polym Sci* 11:57–89.
34. Stofan E, et al. (2013) TiME—The Titan Mare Explorer. *Aerospace Conference IEEE* (IEEE, Piscataway, NJ), pp 1–10.
35. Kresse G, Furthmüller J (1996) Efficient iterative schemes for ab initio total-energy calculations using a plane-wave basis set. *Phys Rev B Condens Matter* 54(16):11169–11186.
36. Kresse G, Joubert D (1999) From ultrasoft pseudopotentials to the projector augmented-wave method. *Phys Rev B* 59(3):1758–1775.
37. Perdew JP, Burke K, Ernzerhof M (1996) Generalized gradient approximation made simple. *Phys Rev Lett* 77(18):3865–3868.
38. Blöchl PE (1994) Projector augmented-wave method. *Phys Rev B Condens Matter* 50(24):17953–17979.
39. Heyd J, Scuseria GE, Ernzerhof M (2003) Hybrid functionals based on a screened Coulomb potential. *J Chem Phys* 118(18):8207–8215.
40. Izmaylov AF, Scuseria GE, Frisch MJ (2006) Efficient evaluation of short-range Hartree-Fock exchange in large molecules and periodic systems. *J Chem Phys* 125(10):104103.
41. Heyd J, Scuseria GE (2004) Efficient hybrid density functional calculations in solids: Assessment of the Heyd-Scuseria-Ernzerhof screened Coulomb hybrid functional. *J Chem Phys* 121(3):1187–1192.
42. Chai J-D, Head-Gordon M (2008) Long-range corrected hybrid density functionals with damped atom-atom dispersion corrections. *Phys Chem Chem Phys* 10(44):6615–6620.
43. Frisch MJ, et al. (2004) *Gaussian 03, Revision D.01* (Gaussian, Inc., Wallingford, CT).
44. Wang Y, Lv J, Zhu L, Ma Y (2012) CALYPSO: A method for crystal structure prediction. *Comput Phys Commun* 183(10):2063–2070.
45. Parlinski K, Li ZQ, Kawazoe Y (1997) First-principles determination of the soft mode in cubic ZrO₂. *Phys Rev Lett* 78(21):4063–4066.
46. Togo A, Tanaka I (2015) First principles phonon calculations in materials science. *Scr Mater* 108:1–5.
47. Deringer VL, Tchougréeff AL, Dronskowski R (2011) Crystal orbital Hamilton population (COHP) analysis as projected from plane-wave basis sets. *J Phys Chem A* 115(21):5461–5466.
48. Maintz S, Deringer VL, Tchougréeff AL, Dronskowski R (2013) Analytic projection from plane-wave and PAW wavefunctions and application to chemical-bonding analysis in solids. *J Comput Chem* 34(29):2557–2567.
49. Towns J, et al. (2014) XSEDE: Accelerating scientific discovery. *Comput Sci Eng* 16:62–74.